

Using Convolutional Neural Networks to detect Edge Localized Modes in DIII-D from Doppler Backscattering measurements

N.Q.X. Teo,^{1,2} V.H. Hall-Chen,¹ K. Barada,³ R.J.H. Ng,¹ L. Gu,⁴ A.K. Yeoh,^{5,1} Q.T. Pratt,³ X. Garbet,² and T.L. Rhodes³

¹*IHPC, Agency for Science, Technology and Research (A*STAR), Singapore*

²*Nanyang Technological University, Singapore*

³*Department of Physics and Astronomy, University of California, Los Angeles, USA*

⁴*RIKEN AIP, Japan*

⁵*Department of Physics, University of Oxford, UK*

(Dated: 4 June 2024)

In H-mode tokamak plasmas, the plasma is sometimes ejected beyond the edge transport barrier. These events are known as edge localized modes (ELMs). ELMs cause a loss of energy and damage the vessel walls. Understanding the physics of ELMs and by extension, how to detect and mitigate them, is an important challenge. In this paper, we focus on two diagnostic methods — D-alpha spectroscopy and Doppler backscattering (DBS). The former detects ELMs by measuring Balmer alpha emission while the latter uses microwave radiation to probe the plasma. DBS has the advantage of having higher temporal resolution and robustness to damage. These advantages of DBS diagnostics may be beneficial for future operational tokamaks and thus data processing techniques for DBS should be developed in preparation. In sight of this, we explore the training of neural networks to detect ELMs from DBS data, using D-alpha data as the ground truth. With shots found in the DIII-D database, the model is trained to classify each time step based on the occurrence of an ELM event. The results are promising. When tested on shots similar to those used for training, the model is capable of consistently achieving a high f1-score of 0.93. This score is a performance metric for imbalanced datasets that ranges between 0 and 1. We evaluate the performance of our neural network on a variety of ELMs — grassy, suppressed, and wide pedestal — finding broad applicability. Beyond ELMs, our work demonstrates the wider feasibility of applying neural networks to data from DBS diagnostics.

I. INTRODUCTION

Edge localized modes (ELM) are events that occur in H-mode tokamak plasmas where plasma is ejected beyond the edge transport barrier¹. This results in a loss of energy and particles, and can cause damage to the tokamak walls. Diagnostics to detect these events are thus important for current and future tokamaks². Currently, ELMs can be detected using D-alpha spectroscopy³, where the Balmer alpha emission from charge exchange reactions is measured. While not traditionally the primary diagnostic for ELMs detection, ELM signatures have been observed by the Doppler backscattering (DBS)^{4,5} diagnostic which uses microwave radiation to probe the plasma. DBS has the advantage of having higher temporal resolution⁶ and robustness to damage⁷, which may be beneficial for future burning plasmas. However, detecting ELMs from DBS measurements is not straightforward and is labor intensive; as such, there is a need to develop automated tools. This paper explores the use of convolutional neural networks to detect ELMs from DBS data. A model is trained on shots of DBS data using D-alpha data as the ground truth, tasked with classifying each time step based on the occurrence of an ELM. Similar work has been done using Beam Emission Spectroscopy instead of DBS, where a deep neural network was trained to predict the likelihood of ELM crashes⁸.

The aim of this research is to act as a proof-of-concept to demonstrate the ability of neural networks to detect

ELMs from DBS data. Ultimately, the goal is to build tools for detection and prediction of ELMs in the burning plasmas of the next generation of tokamaks.

II. DATA

All data used in this research was obtained from the DIII-D⁹ database.

A. Input Data

Raw DBS data is a time-series waveform with a real and complex components from eight channels, each operating at a different microwave frequency¹⁰. Channels with higher probe frequencies penetrate further into the plasma, measuring perturbations at different depths within the pedestal. Only three channels were used for training and testing, channels 1 (55 GHz), 4 (62.5 GHz), and 7 (72.5 GHz), to minimize model size. This data was preprocessed before being fed to the model. The preprocessing involves performing a discrete fast Fourier transform (DFFT) to the waveform to obtain a power spectrum density (PSD), where each time step contains data of the signal power as a function of frequency. We then smoothed the data by performing a running mean over the frequency domain of each time step as gradient descent converged faster after smoothing. The pre-

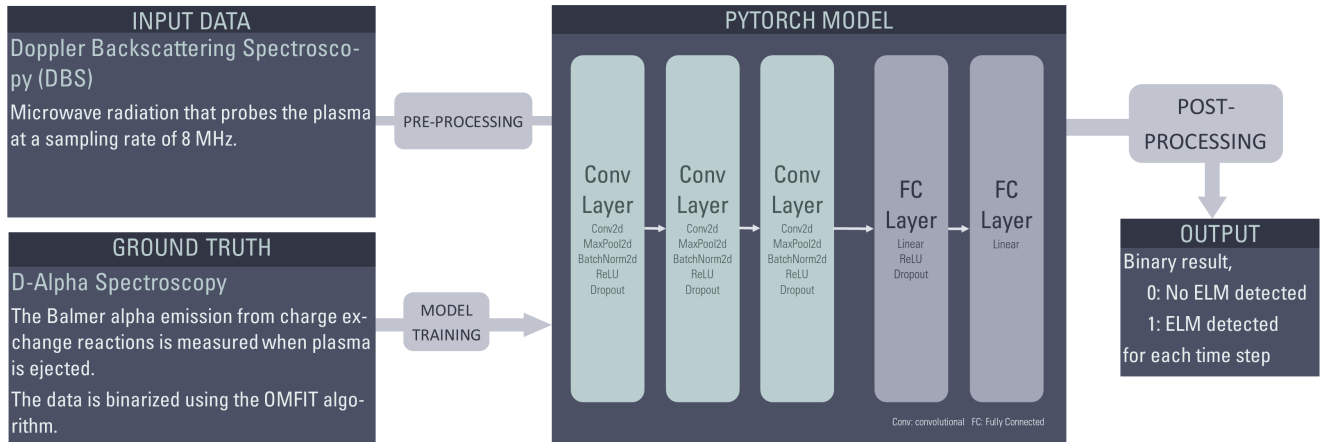


FIG. 1: Diagram of our neural network architecture. The model takes DBS data as input and outputs a binary ELM classification for each time step and is trained using data from D-alpha spectroscopy as the ground truth.

processed data is a 3D array with dimensions of time, channel (probe beam frequency), and Doppler shifted frequency.

B. Ground Truth

The ground truth was obtained from the D-alpha measurement of the shot corresponding to the DBS data. The raw data was binarized using the ELM module in OMFIT^{11,12}, which calls a peak detection script. The output was then resampled to match the time steps of the input data. The final result is a 1D time-series array with 0 representing no ELM event and 1 representing an ongoing ELM event.

III. MODEL

A. Model Architecture

The model is a binary classifier built in the Python library, PyTorch¹³, that classifies each time step of a given DBS PSD (Figure 1). To classify a single time step, the model takes a window of DBS PSD data as input. The window contains DBS data of the current and previous time steps, spanning 128 time steps in total, acting as a form of ‘memory’.

The model contains two main sections — convolutional blocks and a classifier. As the data is simple, the model was designed to be shallow. The data is first fed to three convolutional blocks, containing the following PyTorch layers in order — Conv2d, MaxPool2d, BatchNorm2d, ReLU, and Dropout. The Conv2d layer performs a 2D convolution over the PSD window for each of the three

channels and doubles in size for each subsequent block. MaxPool2d downsamples the data and the ReLU (Rectified Linear Unit) activation function adds non-linearity to the model. BatchNorm2d and Dropout are functions to reduce overfitting, improving generalization of the model. The classifier comprises of the following PyTorch layers in order — Linear, ReLU, Dropout, Linear. The Linear function is a layer where all input and output neurons are linearly connected. Both linear layers are of size 128. The logit output (inverse sigmoid output) passes through a sigmoid function and a rounding function to produce the final binary result. The general model design and structure for this convolutional neural network has been successfully implemented in other research¹⁴ and is hence replicated for this project.

B. Training

Three shots were used for model training: 170869, 170870, and 170878. These shots contain type I ELMs and were recorded at an sampling rate of 8 MHz.

BCEWithLogitsLoss was used as the loss function; it uses binary cross entropy to calculate the loss between the model output and ground truth. Optimization was carried out using the Adam optimizer, incorporating weight decay for regularization. The Adam optimizer is an algorithm that allows for efficient gradient descent during model training. Additionally, the ReduceLRonPlateau scheduler was implemented to dynamically adjust the learning rate in response to stagnant loss values.

Given that the data is in a time-series format and thus inherently ordered, there was no implementation of data shuffling. All training shots were concatenated, and the resultant training dataset was split such that the final 20% of the dataset served as the validation set. With-

out shuffling, the validation set is biased and hence further testing was done on independent shots to assess the model performance.

C. Testing

Initial testing was performed on three shots. These shots contain type I ELMs and were recorded at a sampling rate of 8 MHz. Of these, two are notable and will be discussed, namely 170877 and 170880. The model was also tested on other shots to ascertain its generality. These were either recorded at different sampling rates or contain different ELM types.

Further processing is applied to the model output to improve the model performance. This involves using the running mean of the sigmoid output (output from the sigmoid function applied to the logits) to mitigate small timescale anomalies that are too fast to be consistent with ELM patterns. All parameters used were kept constant for testing to avoid inflating the model performance.

IV. RESULTS

The final model was trained for 23 epochs (training cycles). Two metrics are used to judge the training result: the binary cross entropy loss and the f1-score¹⁵. The f1-score is defined as the harmonic mean of the recall and precision of the model results, ranging from 0, no detection, to 1, perfect detection. The f1 score is an insightful measure of model performance in imbalanced datasets, such as those used in this project (since ELMs are sparse). The final test loss and f1-score is 0.03 and 0.955 respectively and the final validation loss and f1-score is 0.08 and 0.897 respectively. On the training shots, it is unsurprising that the model is capable of reproducing the ground truth well. The f1 score of the processed result is high, above 0.93 for all shots.

The model is capable of reproducing excellent results when tested on shots 170877 and 170880, both achieving f1-scores of 0.93. While the f1-score is an important measure of the model performance, visualization of the model output reveals deeper aspects of the model behaviour. Specific sections of shots are presented in the figures to demonstrate the model behavior as shown in Figure 2. Here, a counting algorithm is introduced to count the number of successfully detected ELM events, along with the false positives and negatives. The algorithm checks every ground truth event for an overlapping model detection. Note that this is only insightful when combined with other performance metrics since a model that predicts all 1s will have detected all events according to the algorithm. For shot 170880, representing lower density ELMs, all 96 ELM events were detected by the model, only differing with the ground truth by the duration of the ELM event. For shot 170877, where ELM density is

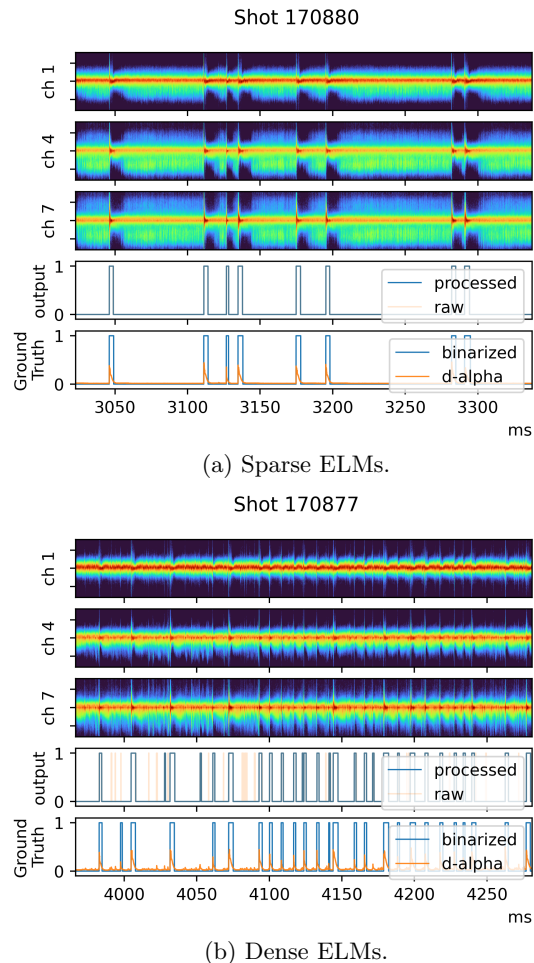


FIG. 2: Testing on shots similar to the training shots yielded excellent results. The plots above show a representative section covering 10% of the entire shot. For shot 170880, every ELM event is detected, where only the duration of each event differing from the ground truth. For denser ELMs in shot 170877, false negatives and positives do appear occasionally.

higher, false positives and negatives occur, albeit infrequently. Of the 153 ELM events, 152 were detected with 11 false positives (7%) and 1 false negative (0.6%). The false positives are generally accompanied by a D-alpha spike that was not sufficiently large to be detected as an ELM event by the OMFIT algorithm. A more meticulous approach in choosing OMFIT parameters may produce a more reliable ground truth data for training and testing. False negatives generally only appear for the processed output, where the raw detection from DBS data is too weak and removed by the post processing algorithm.

On the other hand, testing on DBS data with different characteristics had varying degrees of success (Figure 3). On shot 180866, which contains type I ELMs recorded at a lower sampling rate of 5 MHz, the model produced similarly excellent performance when compared to the

results from shots 170877 and 170880. In the section of shot 180866 shown in Figure 3a, the model achieved an f1-score of 0.94. The model was also tested on three other types of ELMs — grassy (shot 161409), suppressed (shot 154849), and wide-pedestal (shot 169872) ELMs. On these shots, model performance is poorer. While the model was capable of reacting to periods of ELM events, it was not capable of replicating the same model performance. In the section of shots 154849 and 169872, shown in 3c and 3d, the model achieved an f1-score of 0.53 and 0.21 respectively. For grassy ELMs in shot 161409, the D-alpha measurement does not detect any ELM events, making it challenging to ascertain the performance of the model. To solve this, it may be possible to use an infrared thermography diagnostic as a substitute for the ground truth. It should be noted that the f1-scores listed in this paragraph only apply to the section of the shot shown in Figure 3 as shots include other perturbations that are outside the scope of this study, unfairly decreasing the f1-score of the entire shot.

A key observation from these tests is that the signal from channel 7 can be disturbed at certain sections, producing a signal that is not consistent with channels 1 and 4. Since the higher frequency microwave radiation used in channel 7 probes deeper than the other two channels, this observation can be attributed to perturbations in the deeper layers of the plasma. Model performance is greatly affected by these disturbances and as such it may be best not to use higher frequency channels in future training and testing. Alternatively, designing a model to handle such situations (such as voting ensembles) or simply training on more data may produce satisfactory results.

V. DISCUSSION

There are a few immediate steps to improve the current model. Hyperparameter tuning such as random or grid search can be done to improve model performance. Additionally, further training and testing on other types of ELMs should be done. For this to be fruitful, careful selection of shots is needed to ensure the D-alpha data, or any other diagnostic used, is a good representation of the ground truth. Moreover, studies can implement physics-informed components to the model or experiment with liquid neural networks to improve model performance.

Further work can explore models that will be able to predict and label ELMs. This will likely involve adding LSTMs¹⁶ (Long Short Term Memory) or transformers¹⁷ to the model. Another area for development is increasing the speed of the model to enable real-time detection. There are various techniques to achieve this, such as sparsification¹⁸ to reduce the model size.

The ultimate goal is to create tools for future operational tokamaks to detect and, more crucially, predict ELMs through DBS diagnostics. On a more immediate timescale, this research also has the potential to aid cur-

rent researchers in data processing tasks. Models can be developed to process large volumes of data or to identify long period magnetohydrodynamic modes that are laborious to find through human observation.

VI. CONCLUSION

The results of this study are promising. High f1-scores larger than 0.9 are obtained when testing on shots similar to the training shots. The model is also capable of replicating these results on DBS data collected and a different sampling rate. Further work is needed to generalize the model to different types of ELMs.

ACKNOWLEDGMENTS

This work was funded by the Urban and Green Tech Office, A*STAR, Green Seed Fund C231718014, the National Research Foundation, Singapore, and by JST Moonshot R&D Grant Number JPMJMS2011. This material is also based upon work supported by the U.S. Department of Energy, Office of Science, Office of Fusion Energy Sciences, using the DIII-D National Fusion Facility, a DOE Office of Science user facility, under Awards DEFC02-04ER54698, DE-SC0019005, and DE-SC0019007. We thank A.A. Schekochihin, N.A. Crocker, V.P. Bui, and Z. Yang for useful discussions. N.Q.X. Teo thanks the Nanyang Technological University (NTU) Singapore, CN Yang Scholars Programme, for financial support.

Disclaimer. This report was prepared as an account of work partly sponsored by an agency of the United States Government. Neither the United States Government nor any agency thereof, nor any of their employees, makes any warranty, express or implied, or assumes any legal liability or responsibility for the accuracy, completeness, or usefulness of any information, apparatus, product, or process disclosed, or represents that its use would not infringe privately owned rights. Reference herein to any specific commercial product, process, or service by trade name, trademark, manufacturer, or otherwise does not necessarily constitute or imply its endorsement, recommendation, or favoring by the United States Government or any agency thereof. The views and opinions of authors expressed herein do not necessarily state or reflect those of the United States Government or any agency thereof.

- ¹H. Zohm. *Plasma Physics and Controlled Fusion*, 38(2):105, February 1996.
- ²AW Leonard, A Herrmann, K Itami, J Lingertat, A Loarte, TH Osborne, W Suttrop, ITER Divertor Physics Expert Group, et al. *Journal of nuclear materials*, 266:109–117, 1999.
- ³W. W. Heidbrink, K. H. Burrell, Y. Luo, N. A. Pablant, and E. Ruskov. *Plasma Physics and Controlled Fusion*, 46(12):1855, November 2004.
- ⁴M. Hirsch, E. Holzhauer, J. Baldzuhn, B. Kurzan, and B. Scott. *Plasma Physics and Controlled Fusion*, 43(12):1641, October 2001.
- ⁵K. H. Burrell, K. Barada, X. Chen, A. M. Garofalo, R. J. Groebner, C. M. Muscatello, T. H. Osborne, C. C. Petty, T. L. Rhodes, P. B. Snyder, et al. *Physics of Plasmas*, 23(5), 2016.
- ⁶S. Chowdhury, Neal A. Crocker, W. A. Peebles, T. L. Rhodes, L. Zeng, R. Lantsov, B. Van Compernelle, M. Brookman, R. I. Pinsky, and C. Lau. *Review of Scientific Instruments*, 94(7), 2023.
- ⁷F. A. Volpe. *Journal of Instrumentation*, 12(01):C01094, January 2017.
- ⁸D. R. Smith, S. Joung, K. Gill, B. Geiger, G. Mckee, Z. Yan, and J. Zimmerman. Real-time elm onset prediction with deep neural

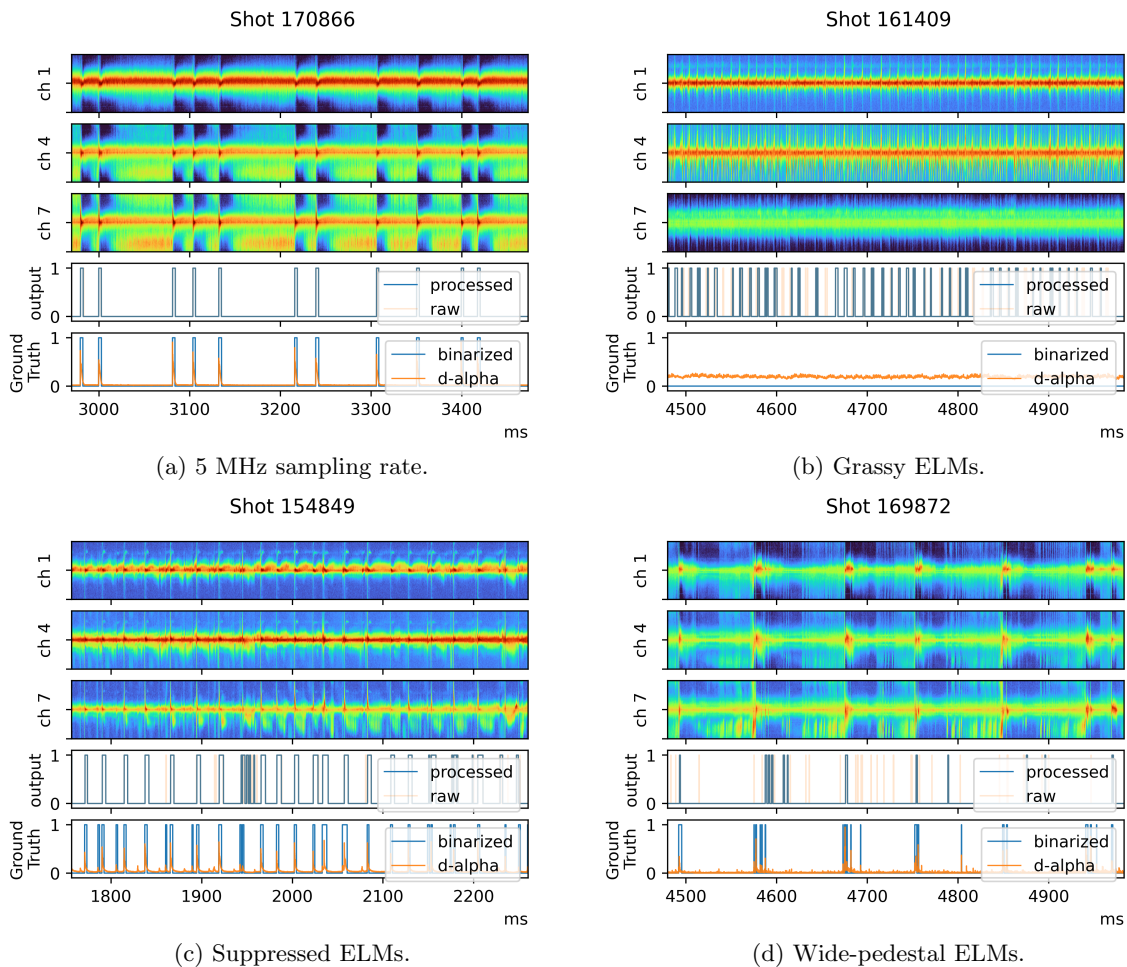


FIG. 3: Applying our model on shots with different parameters and ELM types. We show a representative section covering 10% of the entire shot. When tested on DBS data with a sampling rate of 5 MHz, the model performance is excellent. However, when testing on grassy, suppressed, and wide pedestal ELMs, the model performance is poorer. It should be noted that the D-alpha data for the shot of grassy ELMs is not a good representative of the ground truth. Here, other diagnostics should be explored to substitute D-alpha as the ground truth.

- networks and high-bandwidth edge fluctuation measurements. In Press.
- ⁹R. J. Buttery, T. Abrams, L. Casali, C. M. Greenfield, R. Groebner, C. T. Holcomb, S. Hong, A. Jaervinen, A. Leonard, A. McLean, et al. *Physics of Plasmas*, 30(12), 2023.
- ¹⁰W. A. Peebles, T. L. Rhodes, J. C. Hillesheim, L. Zeng, and C. Wannberg. *Review of Scientific Instruments*, 81(10), 2010.
- ¹¹O. Meneghini and L. Lao. *Plasma and Fusion Research*, 8:2403009–2403009, 2013.
- ¹²O. Meneghini, S. P. Smith, L. L. Lao, O. Izacard, Q. Ren, J. M. Park, J. Candy, Z. Wang, C. J. Luna, V. A. Izzo, et al. *Nuclear Fusion*, 55(8):083008, 2015.
- ¹³A. Paszke, S. Gross, F. Massa, A. Lerer, J. Bradbury, G. Chanan, T. Killeen, Z. Lin, N. Gimelshein, L. Antiga, A. Desmaison, A. Kopf, E. Yang, Z. DeVito, M. Raison, A. Tejani, S. Chilamkurthy, B. Steiner, L. Fang, J. Bai, and S. Chintala. In *Advances in Neural Information Processing Systems 32*, pages 8024–8035. Curran Associates, Inc., 2019.
- ¹⁴M. D. Nguyen, K. Mun, D. Jung, J. Han, M. Park, J. Kim, and J. Kim. In *2020 IEEE International Conference on Consumer Electronics (ICCE)*, pages 1–6. IEEE, 2020.
- ¹⁵L. Alzubaidi, J. Zhang, A. J. Humaidi, A. Al-Dujaili, Y. Duan, O. Al-Shamma, J. Santamaría, M. A. Fadhel, M. Al-Amidie, and L. Farhan. *Journal of big Data*, 8:1–74, 2021.
- ¹⁶G. Van Houdt, C. Mosquera, and G. Nápoles. *Artificial Intelligence Review*, 53(8):5929–5955, 2020.
- ¹⁷D. Soydaner. *Neural Computing and Applications*, 34(16):13371–13385, 2022.
- ¹⁸L. Deng, G. Li, S. Han, L. Shi, and Y. Xie. *Proceedings of the IEEE*, 108(4):485–532, 2020.